Transactions, SMiRT-23
Manchester, United Kingdom - August 10-14, 2015
Division V,Paper ID 823 Modeling Testing and Response Analysis of Structures Systems and Components.

AN EXPERIMENTAL STUDY OF THE IN-PLANE CYCLIC BEHAVIOR OF LOW ASPECT RATIO SC WALL PIERS

Chang-Ching Chang[1], Yin-Nan Huang[2], Bo-An Chen[3], Siamak Epackachi[4], and Andrew Whittaker[5]

[1] Assistant Researcher, National Center for Research on Earthquake Engineering, National Applied Research Laboratories, Taiwan
[2] Associate Professor, Dept. of Civil Engineering, National Taiwan University, Taiwan
[3] Research Assistant, Dept. of Civil Engineering, National Taiwan University, Taiwan
[4] Research Fellow, Dept. of Civil, Structural and Environmental Engineering, University at Buffalo, NY, USA
[5] Professor and Chair, Dept. of Civil, Structural and Environmental Engineering, University at Buffalo, NY, USA

ABSTRACT

A steel-plate-concrete (SC) composite wall is composed of steel faceplates, infill concrete, and connectors. The faceplates are joined with steel tie rods that ensure structural integrity. Steel studs are welded to the faceplates to ensure composite action. This paper summarizes the results of in-plane cyclic tests of four SC walls. The flexure-critical wall piers are two meters long and one meter high. The faceplates are embedded in the foundation and connected to the foundation concrete using shear studs and transverse reinforcement. The influence of infill reinforcement ratio and wall-foundation connection is studied. The test results confirm the effectiveness of the analytical method of Epackachi et al. (2015) in predicting the in-plane monotonic behavior of low aspect-ratio SC wall piers.

INTRODUCTION

Steel-plate-concrete (SC) composite walls are being constructed in nuclear power plants (NPPs) in the United States and China. These walls are composed of steel faceplates, infill concrete, welded connectors that tie the plates together and provide out-of-plane shear reinforcement, and shear studs that enable composite action of the faceplate and the infill concrete and delay buckling of the faceplate. The use of SC walls in safety-related nuclear facilities in Korea, Japan, and the United States has been studied (e.g., Ozaki et al., 2004, Epackachi et al. 2014, Varma et al. 2014) for the past 20 years. Most of numerical studies and test data in the studies of SC walls have focused on the elastic range of response, because NPPs are designed to remain elastic under design basis shaking. Importantly, most of the studies have addressed shear-critical walls because SC walls have been used in the labyrinthine-type of construction used for containment internal structure. The behaviour of flexure- and flexure-shear-critical walls is not as well understood, in part because only a small number of experiments have been performed on such walls.

Epackachi et al. (2014) tested four SC wall piers with an aspect ratio (height divided by length) of 1.0. The piers were anchored to a re-usable foundation block with a post-tensioned connection. A numerical model for SC wall piers was validated using the test data. Epackachi et al. (2015) developed an analytical procedure to predict the flexure and flexure–shear response of SC wall piers using the calibrated numerical model.

This paper addresses the inelastic response of four SC wall piers subjected to reversed, in-plane cyclic loading. The wall-to-foundation connection for these tests is different from that of Epackachi et al. (2014): the faceplates embedded in the foundation using shear studs and transverse reinforcement passed through holes in the faceplates. The following sections of the paper describe the testing program, present key experimental results, and validate the analytical method of Epackachi et al. (2015).

EXPERIMENTAL PROGRAM

Test specimen description

Four wall piers (SC1 through SC4) were constructed and tested under displacement-controlled, reversed cyclic loading. The tests were performed at the National Center for Research on Earthquake Engineering (NCREE) in Taiwan. The design variables considered in the testing program were reinforcement ratio and faceplate slenderness ratio. The aspect ratio (height-to-length, H/L) of all walls was 0.5: one half of the aspect ratio of the Epackachi et al. (2014) specimens. Information on the four walls is provided in Table 1. In this table, studs and tie rods serve as connectors, spaced at distance S; the overall thickness of the wall is T; the thickness of each faceplate is t_p; the reinforcement ratio is $2t_p/T$; and the slenderness ratio of faceplate is S/t_p. No axial load was imposed on the piers. The faceplate slenderness ratios were 17 and 33, where the lower (higher) value complies (does not comply) with the provisions of AISC N690s1 (2015).

Table 1: Test specimen details.

Specimen	Wall dimension ($H \times L \times T$) ($\mathrm{cm} \times \mathrm{cm} \times \mathrm{cm}$)	Stud spacing (cm)	Tie rod spacing (cm)	Reinforcement Ratio (%)	Faceplate slenderness ratio
SC1	$100 \times 200 \times 29.9$	7.5	15	3.1	17
SC2	$100 \times 200 \times 29.9$	-	15	3.1	33
SC3	$100 \times 200 \times 20.9$	7.5	15	4.3	17
SC4	$100 \times 200 \times 20.9$	-	15	4.3	33

Studs and tie rods were used in SC1 and SC3. Only tie rods were used in SC2 and SC4. The diameter of the studs and tie rods was 13 mm for all walls, and they were fabricated from carbon steel with a minimum tensile strength of 1034 MPa (150 ksi). The yield and ultimate strengths of the steel faceplates were 320 MPa and 460 MPa, respectively. The compressive strengths of the infill concrete and the foundation concrete were 30.5 MPa and 42.2 MPa, respectively.

Figure 1 presents an elevation view and cross section of SC1. The base of each wall included a 20-mm thick A572 Gr.50 steel baseplate and nine 10mm-thick stiffeners. They were welded to connect the faceplate and base plate. Two rows of twenty 19-mm diameter headed studs were welded to the baseplate to anchor the faceplate in the foundation and to improve the transfer of shearing and tensile forces. Transverse reinforcement (stirrups) was passed through holes in the embedded sections of the faceplates to further anchor the faceplates. The wall-to-foundation connection was designed to be stiff and strong, and different from the flexible connection used in the Epackachi et al. tests.

Test setup and loading procedure

Figure 2 presents the test setup. Five horizontally inclined, high force-capacity actuators were used to apply quasi-static cyclic lateral loads to each specimen via loading brackets. The foundation block was post-tensioned to the NCREE strong floor with 12 number 69-mm diameter (M69) threaded bars to prevent foundation movement during testing; each M69 bar was posttensioned to 1570 kN. The loading brackets were attached to the specimen using 7 M69 bars post-tensioned to 1570 kN (160 tonnes) per bar.

The displacement-controlled, reversed cyclic loading protocol is presented in Figure 3. Two cycles of loading, with a speed of 0.2 mm/sec, were imposed at each displacement increment. In each loading cycle, a push was exerted first, followed by a pull, where push was defined as the loading in the positive direction to the east (+). Testing was terminated after peak strength had been achieved, at a displacement corresponding to a 30% reduction in resistance.

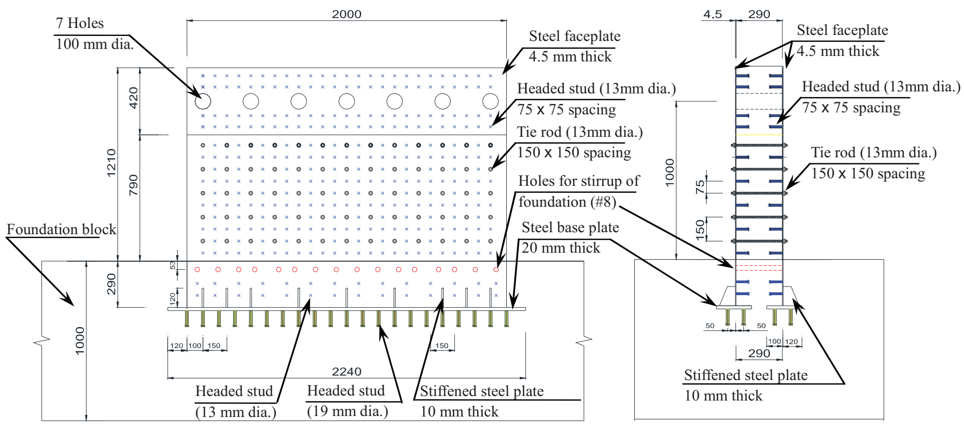

Figure 1. Elevation and cross-section of SC1

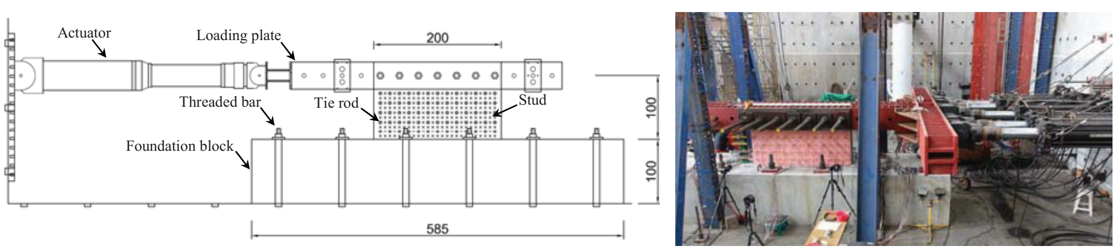

Figure 2. SC wall test setup

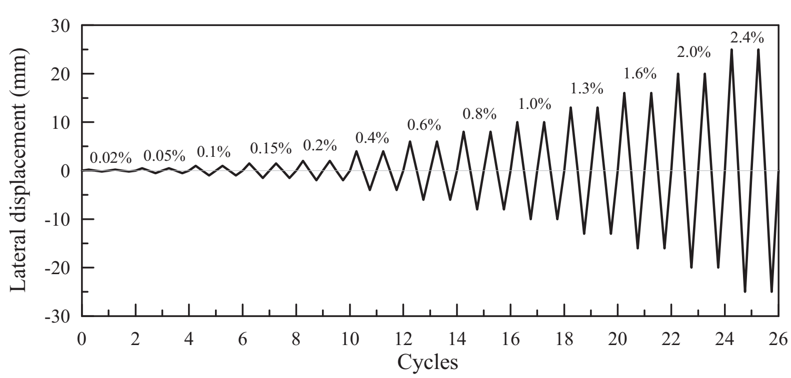

Figure 3. Loading history

Instrumentation

An optical measurement system, strain gauges, linear variable displacement transducers, and dial gauges were used to monitor the response of the wall piers. Linear variable displacement transducers were attached to the ends of the walls to measure in-plane displacement. The movement of the foundation block relative to the strong floor was monitored using dial gauges. The trackers of the optical measurement system were attached to one steel faceplate to measure in-plane and out-of-plane deformations. Strain gauges were installed at four heights above the foundation on the other faceplate to directly measure strains. The locations of the optical trackers and strain gauges are presented in Figure 4.

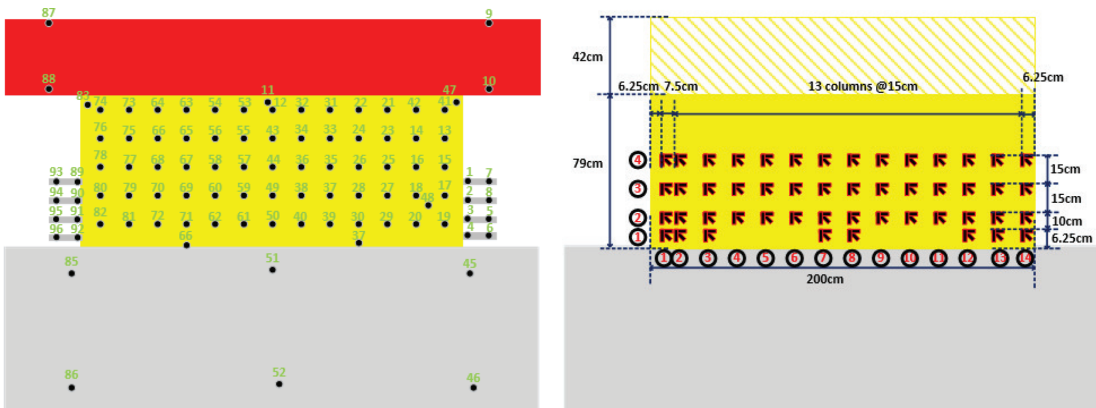

(a) Optical trackers of the optical measurement system (b) Strain gauges

Figure 4. Measuring the strain fields on the faceplates

EXPERIMENTAL RESULTS

Key test results are provided in Table 2 and Figure 5. The initial stiffness of the SC wall piers, calculated at drift angles of less than +0.1%, are presented in the column 2 of Table 2. The values of the displacements corresponding to the onset of faceplate yielding (buckling) are listed in columns 3 and 4 (columns 5 and 6) of Table 2. First yielding of the faceplates was identified using strain gage data. Columns 7 and 8 present the peak loads and the corresponding drift angles in the first (positive) and third (negative) quadrants of Figure 5. Column 9 lists the loads at which the tests were terminated, for both positive (+) and negative (–) directions.

Yielding of the faceplates occurred prior to visible buckling of the faceplates. Buckling of the faceplates first occurred at their free vertical edges prior to achieving peak load. Plate buckling extended towards the center of wall during subsequent cycles of loading and was affected by the connector spacing. Peak loads were observed at a drift angle of +1.1% for SC1, −1% for SC2, −0.7% for SC3, and +1% for SC4. The peak loads developed in SC1 and SC2 (SC3 and SC4) are similar. The faceplate slenderness ratio, of in the range investigated here, did not impact the peak shearing resistance of the specimens.

Table 2: Summary of test results

Specimen	Initial stiffness (kN/mm)	Test data						
		Onset of steel plate yielding		Onset of steel plate buckling		Peak load		Test termination
		Load (kN)	Drift angle (%)	Load (kN)	Drift angle (%)	Load (kN) (+/-)	Drift angle (%) (+/-)	Load (kN) (+/-)
SC1	2063	-2276	-0.16	-3272	-0.67	3450 / -3373	1.1 / -1	1584/-1096
SC2	2016	3294	0.4	-3093	-0.5	3390 / -3498	1.1 / -1	2038/-577
SC3	1981	-2159	-0.14	-3131	-0.69	3074 / -3150	0.56 / -0.7	1640/-779
SC4	1692	2856	0.38	-2813	-0.85	3229 / -3166	1 / -1.5	1684/-1286

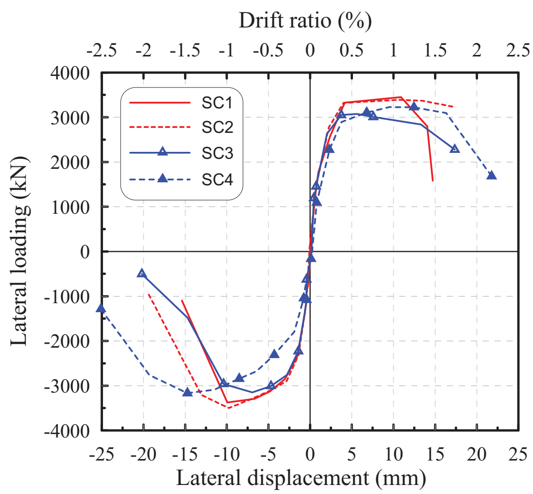

Figure 5. Cyclic backbone curves for the SC walls

Damage to SC walls

Figure 6 illustrates damage to the SC wall piers at the end of testing. The progression of damage in the four SC walls was identical, namely, (1) tensile cracking of the concrete at both ends of the walls, (2) outward buckling and yielding of the steel faceplates at the base of the walls, and (3) crushing and spalling of concrete at the toes of the walls. A steel faceplate was removed from each of SC2 and SC4 for the purpose of documenting damage to the infill concrete. Two wide diagonal cracks formed in the infill concrete and most of the damage to the infill was concentrated immediately above the foundation, at the level of the first row of tie rods.

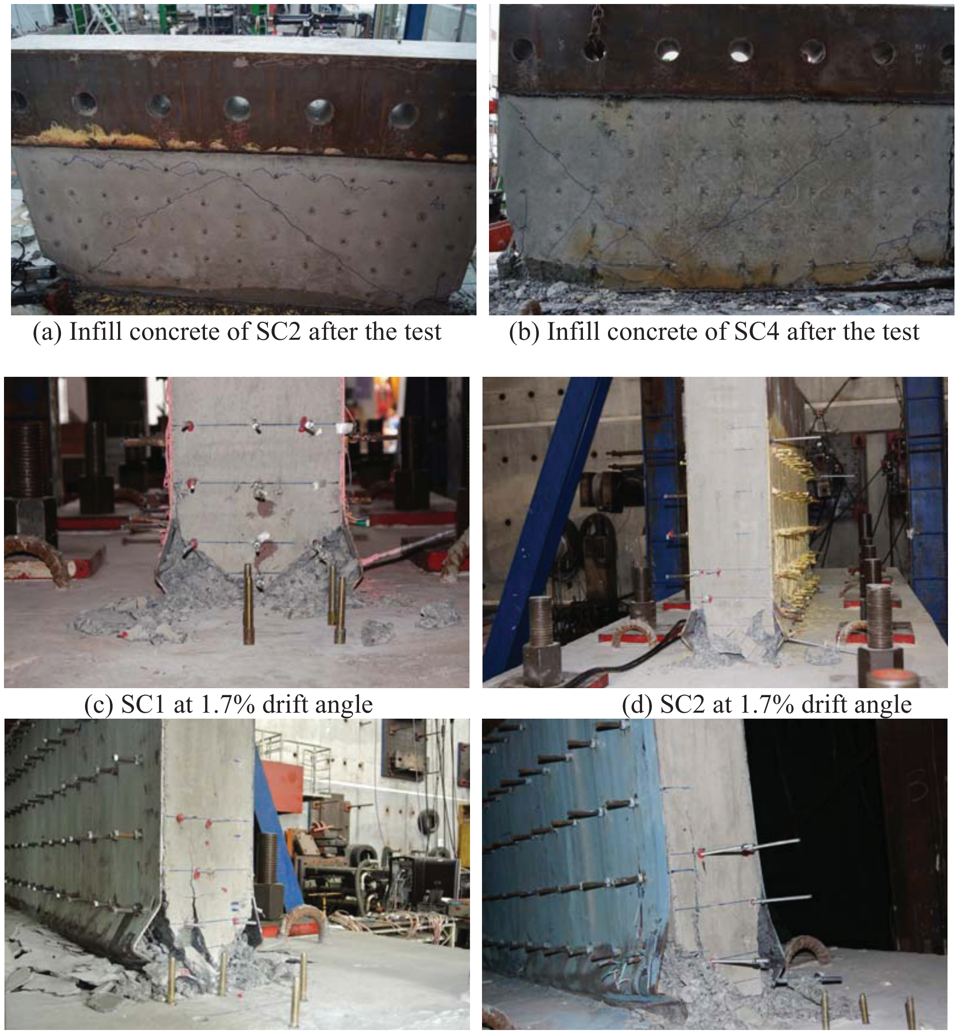

(a) Infill concrete of SC2 after the test (b) Infill concrete of SC4 after the test

(c) SC1 at 1.7% drift angle (d) SC2 at 1.7% drift angle

(e) SC3 at 1.8% drift angle (f) SC4 at 2.2% drift angle

Figure 6. Damage to SC walls

Force-displacement cyclic response

The force-displacement relationships for SC1 through SC4 are presented in Figure 7. Consistent trends were observed regarding the impact of the two tested slenderness ratios of faceplate on hysteresis behavior of SC walls. Pinching is slightly more apparent for the walls with greater slenderness ratio of faceplate.

Negative stiffness was observed in the third quadrant of each panel of Figure 7 and followed by a significant reduction in the strength of the wall in the first quadrant of the panel. When the negative stiffness occurred during the test, damage was observed in the surface of the RC foundation close to the faceplates at the end of the wall further from the actuators, similar to that shown in the lower left corner of panel e of Figure 6. The damage in the foundations greatly influenced the post-peak behavior of the 4 specimens. More discussion can be found in Chang et al. (2015).

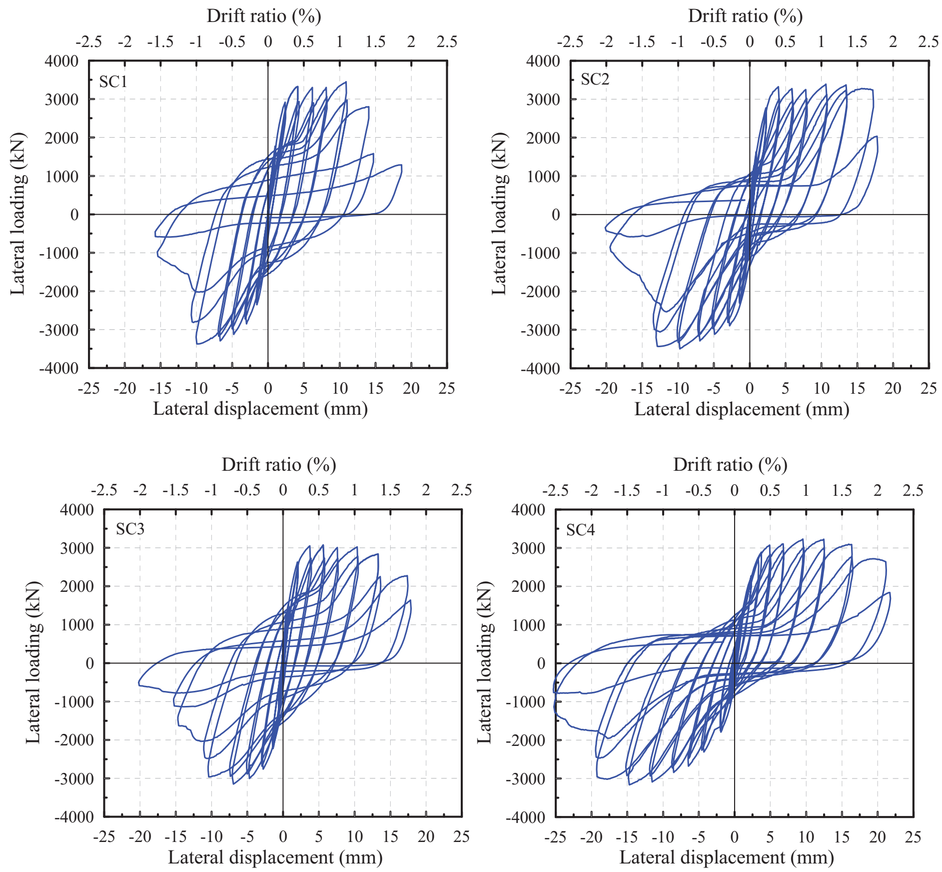

Figure 7. Lateral loading-displacement relationships of SC walls

MONOTONIC ANALYSIS OF SC WALLS

Epackachi et al. (2015) proposed a method to calculate the in-plane flexure-shear response of an SC wall pier subjected to lateral loading. The test results are used to validate the method. The analytical procedure involves eight steps as follows: 1) discretize the wall element into sub-elements along its height and between the points of application of lateral loading (termed a wall panel), 2) calculate the shear force–shear strain relationship for the panel using the equations included in Table 3, 3) calculate the moment–curvature relationship for the cross-sections of the SC wall panel using the equations included in Table 4, 4) modify the moment–curvature relationships of step 2 to account for flexure–shear interaction in the steel faceplates, 5) set the shearing capacity of the panel ($V_t^{\max}$) to the smaller of a) the peak shearing force calculated in step 2 ($V_s^{\max}$), and b) the shearing force corresponding to the flexural strength calculated in step 4 ($V_f^{\max}$), 6) increment the applied shearing force from zero to the shearing capacity of the SC wall calculated in step 5 and calculate the incremental moment applied to each sub-element for each increment of the shearing force, 7) calculate the values of the curvature and shearing strain in each sub-element using the moment–curvature and shearing force–shearing strain relationships calculated in steps 2 and 4. 8) calculate the flexural (Δ_f), shear (Δ_s) and total (Δ_t) displacements corresponding to each increment of the shearing force as

$$\Delta_f = \sum_{i=1}^{m} \phi_i \Delta y_i y_i \tag{1}$$

$$\Delta_s = \sum_{i=1}^{m} \gamma_i \Delta y_i = \gamma_i H \tag{2}$$

$$\Delta_t = \Delta_s + \Delta_f \tag{3}$$

Table 3: Calculation of the shearing response of an SC wall panel (Epackachi et al., 2015)

Limit state	Shearing force (kN)	Shearing stiffness (kN)
Concrete cracking	$V_{cr} = 0.00017\sqrt{f_c^{'}}(A_c + nA_s)$	$K_e = G_s A_s + G_c A_c$
Yielding of the steel faceplate	$V_y = \frac{K_\alpha + K_\beta}{\sqrt{3K_\alpha^2 + K_\beta}} A_s f_y)$	$K_{cr} = K_\alpha + K_\beta$
Concrete crushing	$V_u = \frac{1}{2}\left(\sqrt{1-(\frac{H}{L})^2} + (\eta - 1)\frac{H}{L}\right) A_c f_c^{'}$	$K_y = \frac{V_u + V_y}{0.006 - (\frac{V_{cr}}{K_e} + \frac{V_y + V_{cr}}{K_{cr}})}$
$K_\alpha = G_s A_s$; $K_\beta = \frac{1}{\frac{2(1-v_s)}{A_s E_s} + \frac{4}{A_c E_c^{cr}}}$; $\eta = A_s f_y / A_c f_c^{'}$		

Table 4: Calculation of the flexural response of an SC wall panel. (Epackachi et al., 2015)

Limit state	$\alpha = \frac{c}{L}$	ϕ	M
Concrete cracking	$\alpha_{cr} = \frac{L}{2}$	$\phi_{cr} = \frac{2f_r}{LE_c}$	$M = \frac{f_r L}{6}(A_c + nA_s))$
Yielding of the steel faceplate on tension side of the wall	$\alpha_y^t = \frac{\sqrt{\rho'}}{\sqrt{\rho'+1} + \sqrt{\rho'}}$; $L_y^t = L(\frac{2\alpha^3 - 3\alpha^2 - \rho'}{12\rho'(\alpha - 1)})$	$\phi_y^t = \frac{\varepsilon_y}{L(1-\alpha)}$	$M_y^t = A_s f_y^e L_y^t$
Yielding of the steel faceplate on compressive side of the wall	$\alpha_y^c = \frac{1}{\gamma + 2}$; $L_c^{'} = \alpha L(\frac{1-\beta_2\alpha}{2}), L_s^{'} = \alpha L(1 - \frac{4\alpha}{3})$	$\phi_y^c = \frac{\varepsilon_y}{L\alpha}$	$M_y^c = \beta_1\beta_2 f_c^{'} A_c L_c^{'} + A_s f_s^e L_s^{'}$
Maximum concrete compressive strain equals to ε_{co}	$\alpha_u = \frac{1}{\gamma + 2}$; $L_c^{''} = \alpha L(\frac{1-\beta_2\alpha}{2}), L_s^{''} = \alpha L(1 - \alpha - \frac{\alpha k^2}{3})$	$\phi_u = \frac{\varepsilon_{co}}{L\alpha}$	$M_u = \beta_1\beta_2 f_c^{'} A_c L_c^{''} + A_s f_s^e L_s^{''}$
$\rho' = \frac{2t_s n}{t_c}$; $\gamma = \frac{n\beta_1\beta_2 f_c^{'}}{\rho' f_y}$			

A row of holes was drilled in each faceplate to facilitate construction and this reduced the tensile strength of the faceplates near the base of each wall. The area of the holes is 24% of the cross section area of the faceplate. To apply the Epackachi et al. method, the faceplate thickness was reduced from t_s to $0.76t_s$. Results are presented in Figure 8: the analytical predictions and the experimental measurements are in excellent agreement.

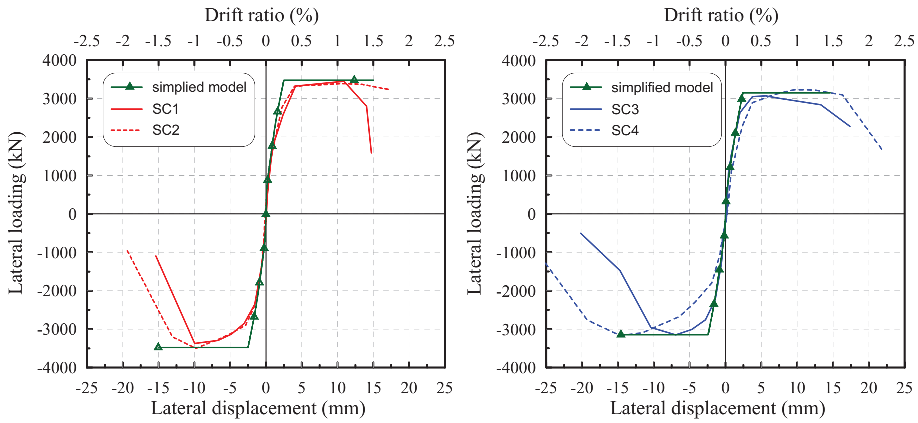

Figure 8. Cyclic backbone curves for the SC walls

CONCLUSION

Four SC wall piers, SC1 through SC4, were constructed and tested under displacement-controlled, reversed cyclic loading at the National Center for Research on Earthquake Engineering in Taiwan. The aspect ratio of each pier was 0.5. The thickness of SC1 and SC2 (SC3 and SC4) was 29.9 (20.9) cm. The faceplate slenderness ratio of SC1 and SC3 (SC2 and SC4) was 17 (33).

Key conclusions of this study are listed as follows:

1. For the two slenderness ratios of faceplate studied herein, SC1 (SC3), the specimen with smaller slenderness ratio, has 1) a peak lateral load capacity similar to SC2 (SC4), and 2) less apparent pinching effect than SC2 (SC4).
2. The wall-foundation design of this study greatly influenced the post-peak hysteresis behavior of SC1 through SC4.
3. The four wall piers of this study sustained peak loads close to those calculated using the analytical method of Epackachi et al. (2015).

ACKNOWLEDGMENTS

The research presented in this paper was supported in part by a grant from National Center for Research on Earthquake Engineering, Taiwan and a grant from the Ministry of Science and Technology of Taiwan under grant MOST 103-2221-E-002-073. The support is gratefully acknowledged.

REFERENCES

AISC (2015). ”Specification for safety-related steel structures for nuclear facilities, Supplement No. 1.” N690s1, American Institute of Steel Construction, Chicago, IL.

Chang, C.-C., Huang, Y.-N., Chen, B.-A., Epackachi, S., and Whittaker, A. S. (2015). "An experimental study of the in-plane cyclic behavior of low-aspect-ratio steel-plate composite wall piers." paper in preparation.

Epackachi, S., Nguyen, N. H., Kurt, E. G., Whittaker, A. S., Varma, A. H. (2014). “In-plane seismic behaviour of rectangular steel-plate composite wall piers.” *Journal of Structural Engineering.* http://dx.doi.org/10.1061/(ASCE)ST.1943-541X.0001148.

Epackachi, S., Whittaker, A. S., and Huang, Y.-N. (2015). "Analytical modeling of rectangular SC wall panels." *Journal of Constructional Steel Research*, 105 49-59.

Ozaki, M., Akita, S., Osuga, H., Nakayama, T., Adachi, N. (2004). “Study on steel plate reinforced concrete panels subjected to cyclic in-plane shear.” *Nuclear Engineering and Design*, 228 225–244.

Varma, A. H., Malushte, S., Sener, K., Lai, Z., (2014). “Steel-plate composite (SC) walls for safety-related nuclear facilities: design for in-plane force and out-of-plane moments.” *Nuclear Engineering and Design*, 269 240-249